Chapter 2
Modeling and Identification

Assistive upper limb technologies must be applied within a controlled environment in order to ensure safety and comfort across a broad spectrum of patient ability. When using electrical stimulation to assist completion of upper limb reaching movements, this environment may be provided by a passive/orthotic support device such as a simple sling or hinged 'de-weighting' structure, or an active robotic mechanism of which many designs are available [1]. In this chapter a suitable model of the combined human arm and mechanical support is developed that has widespread application across upper limb rehabilitation. This representation will then be used in subsequent chapters for model-based controller development.

2.1 Modeling of the Mechanically Supported Human Arm

Spasticity (velocity-dependent stiffness) is common in stroke and typically produces resistance to arm extension due to overactivity of biceps, wrist and finger flexors, and loss of activity of triceps, anterior deltoid, wrist and finger extensors [2]. For effective upper limb stroke rehabilitation, ES should therefore be provided to assist muscles that have experienced a loss of activity, such as the triceps, anterior deltoid, wrist and finger extensors [2–4]. This is in contrast to overactivity of muscles such as the biceps, wrist and finger flexors, which typically produce a resistance to arm extension as a result of spasticity. Triceps and anterior deltoid are hence often selected for stimulation because they align with the clinical need to increase muscle tone and restore motor control of weakened muscles.

C. Freeman, *Control System Design for Electrical Stimulation in Upper Limb Rehabilitation*, DOI 10.1007/978-3-319-25706-8_2

The relationship between muscle stimulation and subsequent movement is well explored, and sophisticated muscle models exist with multiple attachment points across more than one joint, and movement over complex sliding surfaces [5]. Clear divisions exist between modeling for analysis and for direct model-based control application. The former encompass muscles with multiple attachment points, often biarticular structure, and movement over pre-defined sliding surfaces [5, 6]. However, dynamic models used for experimental motion control must be identifiable and assumptions such as muscles eliciting moments about a single fixed axis offer practical routes for parameter identification. A pragmatic approach appropriate to clinical implementation is therefore taken, with additional simplifications discussed in Sect. 2.2. This opens up routes for both parameter identification and controller derivation that have not yet been possible for more complex models [7].

2.1.1 Human Arm Dynamics

A general dynamic model of the human arm is given by

$$\boldsymbol{B}_h(\boldsymbol{\Phi})\ddot{\boldsymbol{\Phi}} + \boldsymbol{C}_h(\boldsymbol{\Phi}, \dot{\boldsymbol{\Phi}})\dot{\boldsymbol{\Phi}} + \boldsymbol{F}_h(\boldsymbol{\Phi}, \dot{\boldsymbol{\Phi}}) + \boldsymbol{G}_h(\boldsymbol{\Phi}) = \boldsymbol{\tau}(\boldsymbol{u}, \boldsymbol{\Phi}, \dot{\boldsymbol{\Phi}}) \tag{2.1}$$

in which $\boldsymbol{\Phi} = [\phi_1, \ldots, \phi_p]^\top$ is the vector of p joint angles, $\boldsymbol{B}_h(\cdot)$ and $\boldsymbol{C}_h(\cdot)$ are inertial and Coriolis $p \times p$ matrices respectively, and $\boldsymbol{F}_h$ and $\boldsymbol{G}_h$ are frictional and gravitational $p \times 1$ vectors respectively. The term $\boldsymbol{\tau}(\boldsymbol{u}, \boldsymbol{\Phi}, \dot{\boldsymbol{\Phi}})$ comprises the moments generated through application of ES, so that if m muscles are assumed to actuate the upper limb system, $\boldsymbol{u}(t) = [u_1(t), \ldots, u_m(t)]^\top$. The ith element of the muscle torque vector $\boldsymbol{\tau}(\cdot)$ is the sum of moments generated by each of the m muscles that may each impart a moment about the ith joint.

2.1.2 Muscle Selection and Modeling

A well-established model of the moment, $\tau(t)$, generated by applying stimulation, $u(t)$, to a muscle acting about a single joint, $\phi(t)$, is

$$\boldsymbol{\tau}\big(u(t), \phi(t), \dot{\phi}(t)\big) = h(u(t), t) \times \tilde{F}_M\big(\phi(t), \dot{\phi}(t)\big) \tag{2.2}$$

where $h(u(t), t)$ is a Hammerstein structure incorporating a static non-linearity, $h_{IRC}(u(t))$, representing the isometric recruitment curve, cascaded with linear activation dynamics, $h_{LAD}(t)$. The multiplicative term $\tilde{F}_M(\cdot)$ captures the effect of joint angle and angular velocity on the force generated. When multiple joints are actuated by multiple muscles and/or tendons which may each span any subset of joints, then the general expression for the total moment generated about the ith joint is

$$\tau_i = \sum_j^m \left\{ r_{i,j}(\phi_i) \times \tau_{i,j}\left(u_j(t), \phi_i(t), \dot{\phi}_i(t)\right) \right\}, \quad i = 1, \ldots, p$$

$$= \Bigg[\underbrace{r_{i,1}(\phi_i)\tilde{F}_{M,i,1}\left(\boldsymbol{\Phi}(t), \dot{\boldsymbol{\Phi}}(t)\right)}_{F_{M,i,1}\left(\boldsymbol{\Phi}(t), \dot{\boldsymbol{\Phi}}(t)\right)}, \ldots, \underbrace{r_{i,m}(\phi_i)\tilde{F}_{M,i,m}\left(\boldsymbol{\Phi}(t), \dot{\boldsymbol{\Phi}}(t)\right)}_{F_{M,i,m}\left(\boldsymbol{\Phi}(t), \dot{\boldsymbol{\Phi}}(t)\right)} \Bigg] \begin{bmatrix} h_1(u_1(t), t) \\ \vdots \\ h_m(u_m(t), t) \end{bmatrix} \tag{2.3}$$

Here $r_{i,j}(\phi_i) = \frac{\partial E_j(\phi_i)}{\partial \phi_i}$ is the moment arm of the jth muscle with respect to the ith joint, where E is the associated excursion (displacement) [8]. If each muscle length is primarily dependent on a single joint angle, the form $\tilde{F}_{M,i,j}(\boldsymbol{\Phi}, \dot{\boldsymbol{\Phi}}) = \tilde{F}_{M,i,j}(\phi_i, \dot{\phi}_i)$ can be taken, leading to the simplified structure

$$\tau_i = \Bigg[\underbrace{r_{i,1}(\phi_i)\tilde{F}_{M,i,1}\left(\phi_i(t), \dot{\phi}_i(t)\right)}_{F_{M,i,1}\left(\phi_i(t), \dot{\phi}_i(t)\right)}, \ldots, \underbrace{r_{i,m}(\phi_i)\tilde{F}_{M,i,m}\left(\phi_i(t), \dot{\phi}_i(t)\right)}_{F_{M,i,m}\left(\phi_i(t), \dot{\phi}_i(t)\right)} \Bigg] \begin{bmatrix} h_1(u_1(t), t) \\ \vdots \\ h_m(u_m(t), t) \end{bmatrix}. \tag{2.4}$$

It is also possible to include the neuromuscular reflex in the form of an additional dynamic function placed in series with the muscle model. However it is neglected here since ES produces negligible effect on the reflex loop when applied on a macroscopic scale as in the transcutaneous case considered in [9, 10]. It is also worth noting that recent works have shown that Hill-Huxley models [11–13] may be at least as accurate as a Hammerstein structure in representing the activation dynamics [14]. The drawback that their complexity undermines application to control has been countered by the proposal of a Hammerstein-Wiener structure [15], but as yet Hill-Huxley models have not been shown to extend to non-isometric conditions, and have not been used in controller derivation.

2.1.3 Mechanical Support

As stated, the human arm is often supported by a mechanical device during ES assisted task practice in order to reduce fatigue and provide additional assistance. A general dynamic model of the support structure which assumes rigid links is

$$\boldsymbol{B}_a(\boldsymbol{\Theta})\ddot{\boldsymbol{\Theta}} + \boldsymbol{C}_a(\boldsymbol{\Theta}, \dot{\boldsymbol{\Theta}})\dot{\boldsymbol{\Theta}} + \boldsymbol{F}_a(\boldsymbol{\Theta}, \dot{\boldsymbol{\Theta}}) + \boldsymbol{G}_a(\boldsymbol{\Theta}) + \boldsymbol{K}_a(\boldsymbol{\Theta}) = -\boldsymbol{J}_a^\top(\boldsymbol{\Theta})\boldsymbol{h} \tag{2.5}$$

where $\boldsymbol{\Theta} = [\theta_1, \ldots, \theta_q]^\top$ is a vector of q joint angles, $\boldsymbol{h}$ is a $q \times 1$ vector of externally applied force, and $\boldsymbol{B}_a(\cdot)$ and $\boldsymbol{C}_a(\cdot)$ are $q \times q$ inertial and Coriolis matrices respectively. In addition, $\boldsymbol{J}_a(\cdot)$ is the system Jacobian, and $\boldsymbol{F}_a(\cdot)$ and $\boldsymbol{G}_a(\cdot)$ are friction and gravitational $q \times 1$ vectors respectively. Finally, vector $\boldsymbol{K}_a(\cdot)$ comprises the $q \times 1$

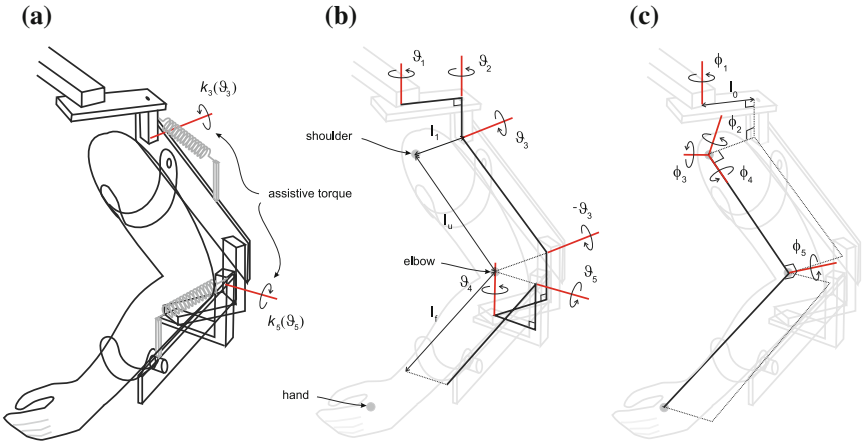

Fig. 2.1 ArmeoSpring: **a** mechanical support, **b** kinematic relationships, and **c** human arm

moments produced by the assistive action of the support mechanism. This may be passive, via springs or counter-balances, or active, as in the case of a robotic structure supplying active torque to assist, or even resist, the intended movement.

A popular form of support is an exoskeletal structure which enables assistance to be applied about individual joints. An example is the commercial ArmeoSpring (Hocoma AG) which provides adjustable force against gravity via two springs. Each joint is aligned in either the horizontal or vertical plane, as shown in Fig. 2.1a, with measured joint variables $\boldsymbol{\Theta} = [\theta_1, \theta_2, \theta_3, \theta_4, \theta_5]^\top$. The patient's arm is rigidly strapped to the exoskeleton support with lengths l_0, l_1 relating the shoulder joint to a fixed base frame.

Hence for the ArmeoSpring $\boldsymbol{B}_a(\cdot)$ and $\boldsymbol{C}_a(\cdot)$ are 5-by-5 inertial and Corelis matrices, and moments produced through gravity compensation provided by each spring yield the form $\boldsymbol{K}_a(\cdot) = [0, 0, k_3(\theta_3), 0, k_5(\theta_5)]^\top$. Figure 2.1c shows the axes corresponding to anthropomorphic joints.

Another common structure is the end-effector type where support is only supplied at a single attachment point. An example is the SaeboMAS (Saebo, Charlotte, USA) shown in Fig. 2.2. Here the support takes the form $\boldsymbol{K}_a(\cdot) = [k_1(\theta_1), 0, 0, 0]^\top$.

2.1.4 Combined Dynamics

It is now assumed that within the necessary joint ranges there exists a unique bijective transformation between coordinate sets, given by $\boldsymbol{\Theta} = \boldsymbol{k}(\boldsymbol{\Phi})$, which allows the mechanical support and human arm models to be combined. This explicitly holds for exoskeletal passive or robotic structures (where $q = p$), and can be extended to

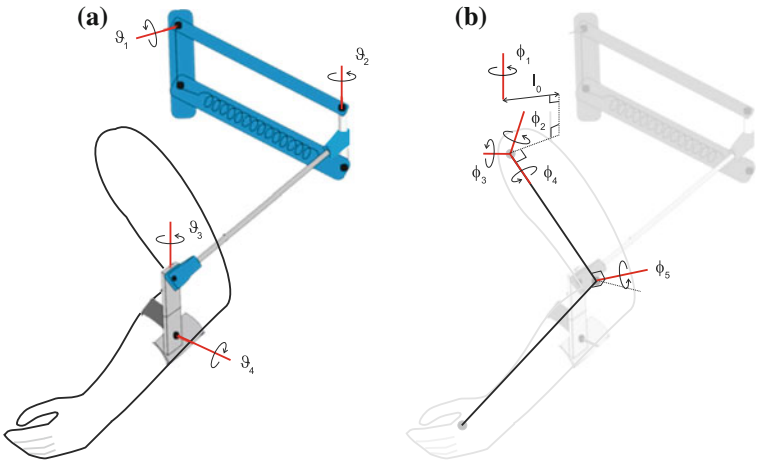

Fig. 2.2 SaeboMAS: **a** mechanical support and kinematic relationships, and **b** human arm

end-effector robot devices developed for rehabilitation. The Lagrangian equation in one variable can be expressed in terms of the other through application of the chain rule, and the results added to produce the combined model

$$\boldsymbol{B}(\boldsymbol{\Phi})\ddot{\boldsymbol{\Phi}} + \boldsymbol{C}(\boldsymbol{\Phi}, \dot{\boldsymbol{\Phi}})\dot{\boldsymbol{\Phi}} + \boldsymbol{F}(\boldsymbol{\Phi}, \dot{\boldsymbol{\Phi}}) + \boldsymbol{G}(\boldsymbol{\Phi}) + \boldsymbol{K}(\boldsymbol{\Phi}) = \boldsymbol{\tau}(\boldsymbol{u}, \boldsymbol{\Phi}, \dot{\boldsymbol{\Phi}}) - \boldsymbol{J}^{\top}(\boldsymbol{\Phi})\boldsymbol{h} \tag{2.6}$$

where

$$\begin{aligned}
\boldsymbol{B}(\boldsymbol{\Phi}) &= \boldsymbol{B}_h(\boldsymbol{\Phi}) + \boldsymbol{k}_1(\boldsymbol{\Phi})^{\top}\boldsymbol{B}_a(\boldsymbol{k}(\boldsymbol{\Phi}))\boldsymbol{k}_1(\boldsymbol{\Phi}), \quad \boldsymbol{J}^{\top}(\boldsymbol{\Phi}) = \boldsymbol{k}_1(\boldsymbol{\Phi})^{\top}\boldsymbol{J}_a^{\top}(\boldsymbol{k}(\boldsymbol{\Phi})), \\
\boldsymbol{C}(\boldsymbol{\Phi}, \dot{\boldsymbol{\Phi}}) &= \boldsymbol{C}_h(\boldsymbol{\Phi}, \dot{\boldsymbol{\Phi}}) + \boldsymbol{k}_1(\boldsymbol{\Phi})^{\top}\boldsymbol{C}_a(\boldsymbol{k}(\boldsymbol{\Phi}), \boldsymbol{k}_1(\boldsymbol{\Phi})\dot{\boldsymbol{\Phi}})\boldsymbol{k}_1(\boldsymbol{\Phi}) \\
&\quad + \boldsymbol{k}_1(\boldsymbol{\Phi})^{\top}\boldsymbol{B}_a(\boldsymbol{k}(\boldsymbol{\Phi}))\boldsymbol{k}_2(\boldsymbol{\Phi}, \dot{\boldsymbol{\Phi}}), \\
\boldsymbol{F}(\boldsymbol{\Phi}, \dot{\boldsymbol{\Phi}}) &= \boldsymbol{F}_h(\boldsymbol{\Phi}, \dot{\boldsymbol{\Phi}}) + \boldsymbol{k}_1(\boldsymbol{\Phi})^{\top}\boldsymbol{F}_a(\boldsymbol{k}(\boldsymbol{\Phi}), \boldsymbol{k}_1(\boldsymbol{\Phi})\dot{\boldsymbol{\Phi}}), \quad \boldsymbol{K}(\boldsymbol{\Phi}) = \boldsymbol{k}_1(\boldsymbol{\Phi})^{\top}\boldsymbol{K}_a(\boldsymbol{k}(\boldsymbol{\Phi})), \\
\boldsymbol{G}(\boldsymbol{\Phi}) &= \boldsymbol{G}_h(\boldsymbol{\Phi}) + \boldsymbol{k}_1(\boldsymbol{\Phi})^{\top}\boldsymbol{G}_a(\boldsymbol{k}(\boldsymbol{\Phi})),
\end{aligned}$$

with $\boldsymbol{k}_1(\boldsymbol{\Phi}) = \dfrac{d\boldsymbol{k}(\boldsymbol{\Phi})}{d\boldsymbol{\Phi}}$ and $\boldsymbol{k}_2(\boldsymbol{\Phi}, \dot{\boldsymbol{\Phi}}) = \dfrac{d}{dt}\left(\dfrac{d\boldsymbol{k}(\boldsymbol{\Phi})}{d\boldsymbol{\Phi}}\right)$.

Now let each $h_{LAD,j}(t)$ be realized using continuous-time state-space model matrices $\{\boldsymbol{M}_{A,j}, \boldsymbol{M}_{B,j}, \boldsymbol{M}_{C,j}\}$ (state, input and output respectively), with corresponding states $\boldsymbol{x}_j(t)$. The system (2.6) can then be expressed over time interval $t \geq 0$ in the following state-space form

$$\dot{\boldsymbol{x}}_s(t) = \underbrace{\begin{bmatrix} \dot{\boldsymbol{\Phi}}(t) \\ \boldsymbol{B}(\boldsymbol{\Phi}(t))^{-1}\boldsymbol{X}\left(\boldsymbol{\Phi}(t), \dot{\boldsymbol{\Phi}}(t)\right) \\ \boldsymbol{M}_{A,1}\boldsymbol{x}_1 \\ \vdots \\ \boldsymbol{M}_{A,m}\boldsymbol{x}_m \end{bmatrix}}_{\boldsymbol{f}_s(\boldsymbol{x}_s(t))} + \underbrace{\begin{bmatrix} \boldsymbol{0} \\ \boldsymbol{0} \\ \boldsymbol{M}_{B,1}h_{IRC,1}(u_1(t)) \\ \vdots \\ \boldsymbol{M}_{B,m}h_{IRC,m}(u_m(t)) \end{bmatrix}}_{\boldsymbol{g}_s(\boldsymbol{u}(t))},$$

$$\boldsymbol{\Phi}(t) = \underbrace{\begin{bmatrix} \boldsymbol{I} & \boldsymbol{0} & \cdots & \boldsymbol{0} \end{bmatrix}\boldsymbol{x}_s(t)}_{\boldsymbol{h}_s(\boldsymbol{x}_s(t))}, \quad \boldsymbol{\Phi}(0) = \boldsymbol{\Phi}_0, \tag{2.7}$$

where $\boldsymbol{x}_s(t) = [\boldsymbol{\Phi}(t)^\top, \ \dot{\boldsymbol{\Phi}}(t)^\top, \ \boldsymbol{x}_1(t)^\top \ \cdots \ \boldsymbol{x}_m(t)^\top]^\top$, and the ith row of $\boldsymbol{X}\left(\boldsymbol{\Phi}(t), \dot{\boldsymbol{\Phi}}(t)\right)$ is given by

$$\begin{aligned} X_i\left(\boldsymbol{\Phi}(t), \dot{\boldsymbol{\Phi}}(t)\right) = &\sum_j^m \left(\boldsymbol{M}_{C,j}\boldsymbol{x}_j(t)F_{M,i,j}\left(\boldsymbol{\Phi}(t), \dot{\boldsymbol{\Phi}}(t)\right)\right) - \left(\boldsymbol{J}^\top(\boldsymbol{\Phi}(t))\right)_i \boldsymbol{h}(t) \\ &- \boldsymbol{C}_i\left(\boldsymbol{\Phi}(t), \dot{\boldsymbol{\Phi}}(t)\right)\dot{\boldsymbol{\Phi}}(t) - \boldsymbol{F}_i\left(\boldsymbol{\Phi}(t), \dot{\boldsymbol{\Phi}}(t)\right) - \boldsymbol{G}_i(\boldsymbol{\Phi}(t)) - \boldsymbol{K}_i(\boldsymbol{\Phi}(t)). \end{aligned}$$

2.2 Model Identification

We next develop procedures to identify parameters in composite model (2.6) that can be used in a clinical setting. We first assume it is possible to manipulate each joint individually while measuring and recording the resulting joint angle and applied force signals. This is clearly not possible for all joints in the wrist and hand, and so alternative identification approaches for these structures are presented in Chap. 8.

Depending on the underlying musculo-tendon structure, it is often possible to set terms within (2.3) or (2.4) to zero by defining joint axes which align with the axes about which muscles generate moments. This is discussed next, before an illustrative example is presented in Sect. 2.2.5.

2.2.1 Muscle Axis Identification

After measuring rigid body lengths, the next step is to define the position and orientation of each joint in the kinematic chain of the anthropomorphic system. In some cases these axes are uniquely defined (e.g. the elbow joint) and in others multiple choices are possible (e.g. the glenohumeral joint). In the latter case joints can be specified to align with the one or more axes about which ES produces movement (e.g. motion about the glenohumeral joint due to anterior deltoid stimulation). Identification of these axes is simplified if they can be assumed to be fixed with respect to a rigid link, and a suitable procedure is described in the appendix of [16]. This involves applying stimulation followed by the least squares fitting of a three dimen-

sional plane to the arc traced out by a point attached to the link. Fixed rotations are introduced into the kinematic chain to align the axis with a vector orthogonal to this plane. This procedure results in components of $F_M(\cdot)$ within (2.3) being set to zero. For example, if muscle j is aniarticular (i.e. acts about a single joint axis) and the above approach is applied to identify corresponding joint axis i, this produces the simplified form

$$F_{M,i,j}(\boldsymbol{\Phi}(t), \dot{\boldsymbol{\Phi}}(t)) \begin{cases} =0, & j \neq i \\ \neq 0, & j = i. \end{cases} \tag{2.8}$$

2.2.2 Passive Parameter Identification

With no applied ES, system (2.6) simplifies to

$$\boldsymbol{B}(\boldsymbol{\Phi})\ddot{\boldsymbol{\Phi}} + \boldsymbol{C}(\boldsymbol{\Phi}, \dot{\boldsymbol{\Phi}})\dot{\boldsymbol{\Phi}} + \boldsymbol{F}(\boldsymbol{\Phi}, \dot{\boldsymbol{\Phi}}) + \boldsymbol{G}(\boldsymbol{\Phi}) + \boldsymbol{K}(\boldsymbol{\Phi}) = -\boldsymbol{J}_h^\top(\boldsymbol{\Phi})\boldsymbol{h} \tag{2.9}$$

and can be written in a linear-in-parameter form. First introduce matrix $\boldsymbol{Y}_B$ containing kinematic data, and vector $\boldsymbol{\pi}_B$ containing a minimal parameter set, such that

$$\begin{aligned} &\boldsymbol{Y}_B\left(\boldsymbol{\Phi}(t), \dot{\boldsymbol{\Phi}}(t), \ddot{\boldsymbol{\Phi}}(t)\right)\boldsymbol{\pi}_B \\ &\quad = \boldsymbol{B}(\boldsymbol{\Phi}(t))\ddot{\boldsymbol{\Phi}}(t) + \boldsymbol{C}(\boldsymbol{\Phi}(t), \dot{\boldsymbol{\Phi}}(t))\dot{\boldsymbol{\Phi}}(t) + \boldsymbol{G}(\boldsymbol{\Phi}(t)) + \boldsymbol{K}(\boldsymbol{\Phi}(t)). \end{aligned}$$

Similarly represent $\boldsymbol{F}(\boldsymbol{\Phi}, \dot{\boldsymbol{\Phi}})$ using piecewise linear functions by introducing matrix $\boldsymbol{Y}_F$ containing kinematic data, and vector $\boldsymbol{\pi}_F$ containing a minimal parameter set, such that

$$\boldsymbol{Y}_F\left(\boldsymbol{\Phi}(t), \dot{\boldsymbol{\Phi}}(t)\right)\boldsymbol{\pi}_F = \boldsymbol{F}(\boldsymbol{\Phi}(t), \dot{\boldsymbol{\Phi}}(t)). \tag{2.10}$$

Using these (2.9) is written as

$$\underbrace{[\boldsymbol{Y}_B(t),\ \boldsymbol{Y}_F(t)]}_{\boldsymbol{Y}(t)} \underbrace{\left[\boldsymbol{\pi}_B^\top,\ \boldsymbol{\pi}_F^\top\right]^\top}_{\boldsymbol{\pi}} = \underbrace{-\boldsymbol{J}_h^\top(\boldsymbol{\Phi}(t))\boldsymbol{h}(t)}_{\hat{\boldsymbol{\tau}}(t)}. \tag{2.11}$$

A 6-axis force/torque sensor is attached to the extreme link of the mechanical support to provide externally applied force and torque vector $\boldsymbol{h}$. This can be done using a handle attached to the sensor which is used to kinematically excite the system, during which the kinematic variables $\boldsymbol{Y}(t)$ and forces $\hat{\boldsymbol{\tau}}(t)$ are recorded at discrete times $t = \{t_1, \ldots, t_N\}$. For structures with multiple degrees of freedom, this process may need to be repeated with different attachment points to provide sufficient kinematic excitation to all joints. From these assemble the matrices

$$\bar{\boldsymbol{Y}} = \left[\boldsymbol{Y}(t_1)^\top \cdots \boldsymbol{Y}(t_N)^\top\right]^\top, \quad \bar{\boldsymbol{\tau}} = \left[\hat{\boldsymbol{\tau}}(t_1)^\top \cdots \hat{\boldsymbol{\tau}}(t_N)^\top\right]^\top.$$

The least squares solution to the problem $\min_{\boldsymbol{\pi}} \|\bar{\boldsymbol{Y}}\boldsymbol{\pi} - \bar{\boldsymbol{\tau}}\|^2$ for the parameter vector is $\boldsymbol{\pi} = \bar{\boldsymbol{Y}}^{\dagger}\bar{\boldsymbol{\tau}}$ where $\boldsymbol{A}^{\dagger} = (\boldsymbol{A}^{\top}\boldsymbol{A})^{-1}\boldsymbol{A}^{\top}$ denotes the pseudoinverse of $\boldsymbol{A}$.

There is always a compromise between accuracy and repeatability in practice, and hence the simplest realistic structure should be used to represent unknown functional forms appearing in (2.6). For example, biomechanical coupling between anthropomorphic joints can be omitted to give the form

$$\boldsymbol{F}(\boldsymbol{\Phi}, \dot{\boldsymbol{\Phi}}) = [F_{e,1}(\phi_1) + F_{v,1}(\dot{\phi}_1), \ldots, F_{e,p}(\phi_p) + F_{v,p}(\dot{\phi}_p)]^{\top}, \tag{2.12}$$

provided effects such as spasticity in bi-articular elbow/shoulder muscles are sufficiently mild [17, 18]. The form (2.12) requires p instances of the structure

$$\sum_{n=1}^{N_e} a_n X_n(\phi_i) + \sum_{n=1}^{N_v} b_n X_n(\dot{\phi}_i), \quad i = 1, \ldots, p \tag{2.13}$$

with basis function $X_n(\dot{)}$, and N_e, N_v denoting the number of parameters appearing in each functional form. This gives rise to vector $[a_1, \ldots, a_{N_e}, b_1, \ldots, b_{N_v}]$ appearing in $\boldsymbol{\pi}_F$ for each instance, and a total of $p \times (N_e + N_v)$ parameters. Taking the more general form

$$\boldsymbol{F}(\boldsymbol{\Phi}, \dot{\boldsymbol{\Phi}}) = [F_{ev,1}(\phi_1, \dot{\phi}_1), \ldots, F_{ev,p}(\phi_p, \dot{\phi}_p)]^{\top}, \tag{2.14}$$

requires p instances of the form

$$\sum_{n=1}^{N_e \times N_v} c_n X_n(\phi_i, \dot{\phi}_i), \quad i = 1, \ldots, p \tag{2.15}$$

and hence a total of $p \times (N_e \times N_v)$ parameters appear in $\boldsymbol{\pi}_F$. More general functional forms therefore require far more data to identify, with the most general structure requiring $p^2 \times N_e \times N_v$ parameters. The simpler form of (2.12) has been found to be accurate provided effects such as spasticity in bi-articular elbow/shoulder muscles, which introduce biomechanical coupling between joints, are sufficiently mild [17]. Further information on constructing basis functions appears in [18].

2.2.3 Muscle Identification

Next consider the Hammerstein structures $h_j(u_j, t)$, $j = 1, \ldots, m$ appearing in torque vector $\boldsymbol{\tau}(t)$, defined by (2.2). These are identified by fixing the sensor handle and applying ES inputs, $u_j(t)$, to each muscle in turn. Vector $\hat{\boldsymbol{\tau}}(t)$ is recorded and the torque generated about the ith joint axis is extracted using

$$\tau_{i,j}(u_j(t), \boldsymbol{\Phi}, \dot{\boldsymbol{\Phi}}) = \boldsymbol{Y}_i(t)\hat{\boldsymbol{\pi}} - \hat{\tau}_i, \quad i = 1, \ldots, p \tag{2.16}$$

where $\hat{\boldsymbol{\pi}}$ is provided by the previous tests. Here $\boldsymbol{Y}_i(t)$ corresponds to static operating conditions $\boldsymbol{\Phi} = \bar{\boldsymbol{\Phi}}$, $\dot{\boldsymbol{\Phi}}, \ddot{\boldsymbol{\Phi}} = \mathbf{0}$, and taking without loss of generality $F_{M,i,j}(\bar{\boldsymbol{\Phi}}, \mathbf{0}) = 1$,

$$\tau_{i,j}(u_j(t), \bar{\boldsymbol{\Phi}}, \mathbf{0}) = h_j(u_j, t) \times F_{M,i,j}(\bar{\boldsymbol{\Phi}}, \mathbf{0}) = h_j(u_j, t). \tag{2.17}$$

Algorithms developed specifically for stroke patients appear in [19], and can be applied to data sets $\{u_j, \tau_{i,j}(\cdot)\}_{i=1,\ldots,p}$ to identify the Hammerstein structures $h_j(u_j, t)$, $j = 1, \ldots, m$. Each of these comprises static nonlinearity $h_{IRC,j}(\cdot)$ and linear activation dynamics $h_{LAD,j}(\cdot)$. The latter is then expressed using state-space matrices $\boldsymbol{M}_{A,j}$, $\boldsymbol{M}_{B,j}$, $\boldsymbol{M}_{C,j}$ for inclusion in state-space form (2.7).

2.2.4 Multiplicative Muscle Function Identification

To identify the general form of muscle function $F_{M,i,j}(\boldsymbol{\Phi}(t), \dot{\boldsymbol{\Phi}}(t))$, kinematic excitation is again applied and $\boldsymbol{Y}(t)$ and $\hat{\boldsymbol{\tau}}(t)$ recorded at samples $t = \{t_1, \ldots, t_N\}$. However now ES sequences $u_j(t)$ are applied and using the Hammerstein models previously identified, the isometric muscle torque is calculated using $h_j(u_j, t)$, so that

$$F_{M,i,j}(\boldsymbol{\Phi}(t), \dot{\boldsymbol{\Phi}}(t)) = \frac{\tau_i^*(t) - \hat{\tau}_i(t)}{h_j(u_j(t), t)}, \quad j = 1, \ldots, m. \tag{2.18}$$

Here $\boldsymbol{\tau}^*(t) = \boldsymbol{Y}(t)\hat{\boldsymbol{\pi}}$ is the passive torque, with $\hat{\boldsymbol{\pi}}$ provided by previous tests. $F_{M,i,j}(\cdot)$ is now represented as $\boldsymbol{Y}_{F_M}(t)\boldsymbol{\pi}_{F_m}$, with an optimal parameter set $\boldsymbol{\pi}_{F_M} = \bar{\boldsymbol{Y}}^{\dagger}\bar{\boldsymbol{\tau}}$, where

$$\bar{\boldsymbol{Y}} = \begin{bmatrix} \boldsymbol{Y}_{F_M}(t_1) \\ \vdots \\ \boldsymbol{Y}_{F_M}(t_N) \end{bmatrix}, \quad \bar{\boldsymbol{\tau}} = \begin{bmatrix} \dfrac{\tau_i^*(t_1) - \hat{\tau}_i(t_1)}{h_j(u_j(t_1), t_1)} \\ \vdots \\ \dfrac{\tau_i^*(t_N) - \hat{\tau}_i(t_N)}{h_j(u_j(t_N), t_N)} \end{bmatrix}.$$

Given the limited time available for identification in a clinical setting, accuracy can be improved by taking the simplest structure capable of capturing the underlying relationship. For example, if muscle length can be assumed to predominantly depend on a single joint angle, structure (2.4) yields

$$F_{M,i,j}(\boldsymbol{\Phi}(t), \dot{\boldsymbol{\Phi}}(t)) = F_{M,i,j}(\phi_i(t), \dot{\phi}_i(t)), \quad j = 1, \ldots, m \tag{2.19}$$

giving rise to m instances of the form (2.15), and a total of $m \times (N_e \times N_v)$ parameters, each associated with kinematic excitation of a single variable. To produce more

repeatable muscle functions, it has been proposed in [20] that the muscle model function takes the form

$$F_{M,i,j}(\boldsymbol{\Phi}(t), \dot{\boldsymbol{\Phi}}(t)) = F_{M1,i,j}(\phi_i(t)) \times F_{M2,i,j}(\dot{\phi}_i(t)), \quad j = 1, \ldots, m \tag{2.20}$$

and taking logarithms produces the identifiable form

$$\log\left(F_{M1,i,j}(\phi_i(t))\right) + \log\left(F_{M2,i,j}(\dot{\phi}_i(t))\right) = \log\left(\frac{\tau_i^*(t) - \hat{\tau}_i(t)}{h_j(u_j(t), t)}\right) \tag{2.21}$$

reducing the number of parameters to m instances of form (2.13) with a total of only $m \times (N_e + N_v)$ parameters. After identification, functions $F_{M1,i,j}(\phi_i(t))$ and $F_{M2,i,j}(\dot{\phi}_i(t))$ are retrieved through application of the exponential function.

2.2.5 *Case Study: Triceps and Anterior Deltoid with ArmeoSpring*

Consider the combined anthropomorphic and mechanical support structure shown in Fig. 2.1 and assume that ES is applied to the triceps and the anterior deltoid muscles. Following the procedure of Sect. 2.2.1, we assume the triceps generates a moment about an axis orthogonal to both the forearm and upper arm, and that the anterior deltoid generates a moment about an axis that is fixed with respect to the shoulder. These axes are shown in Fig. 2.3.

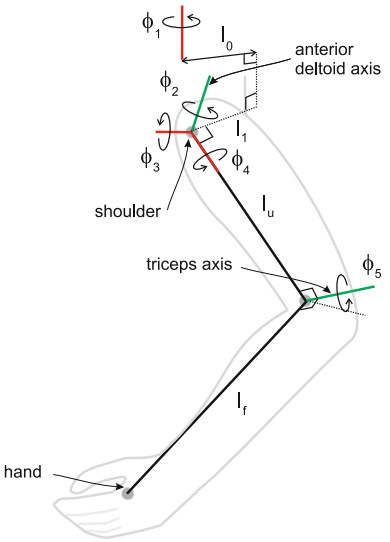

Fig. 2.3 Human arm kinematic relatioships ($m = 2$, $p = 5$)

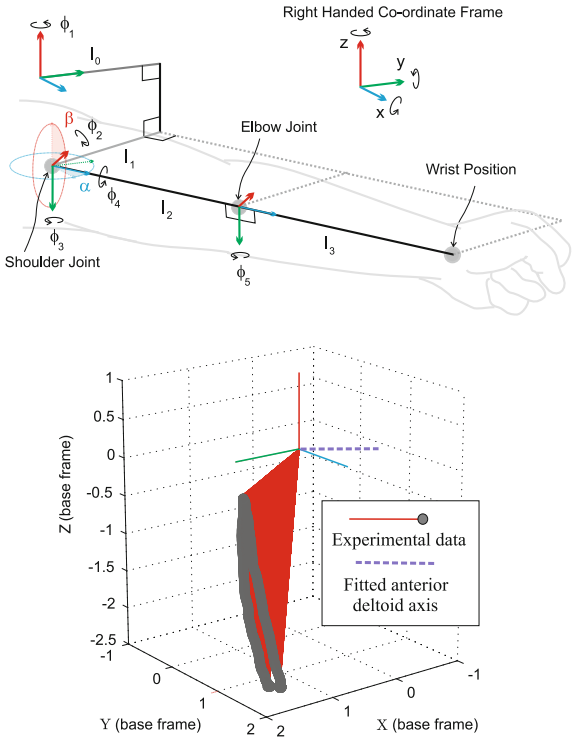

Fig. 2.4 Kinematic model with α and β defining the anterior deltoid axis, together with fitted experimental data. Experimental values $\alpha = 8°$, $\beta = -87°$, are shown together with $\phi_1 = \phi_2 = \phi_3 = \phi_4 = \phi_5 = 0$

To identify the anterior deltoid axis experimentally, the participant is seated in the ArmeoSpring, which is adjusted to their individual arm dimensions. The level of support in each spring is modified so that their arm is raised above their lap. Surface electrodes are placed on the anterior deltoid and triceps muscles and adjusted to elicit the maximum appropriate movement. ES is then applied to the anterior deltoid using a trapezoidal profile to slowly lift the arm, and then lower it back to the starting position. To orientate the ϕ_2 axis to correspond with the stimulated anterior deltoid, two additional rotations, with variables α and β, are introduced as shown in Fig. 2.4. After initial rotation of the base frame by ϕ_1, it is rotated about the z-axis by α and about the x-axis by β. The identification procedure described in the appendix of [16] yields values of α and β which are then substituted into the augmented dynamic model. An example of the fitted axis is shown in Fig. 2.4.

Next the passive identification procedure of Sect. 2.2.2 is applied using the functional form (2.12), yielding the parameter vector $\boldsymbol{\pi}$ appearing in (2.11). Examples of resulting frictional parameters relating to joint ϕ_2 are shown in Fig. 2.5.

The muscle identification procedure described in Sect. 2.2.3 is then applied. Experimental results are shown in Fig. 2.6 where the forms

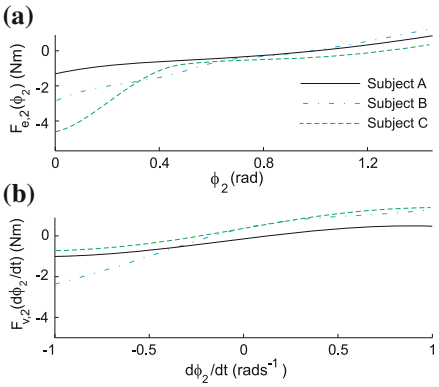

Fig. 2.5 Identified forms **a** $F_{e2}(\phi_2)$ and **b** $F_{v2}(\dot{\phi}_2)$

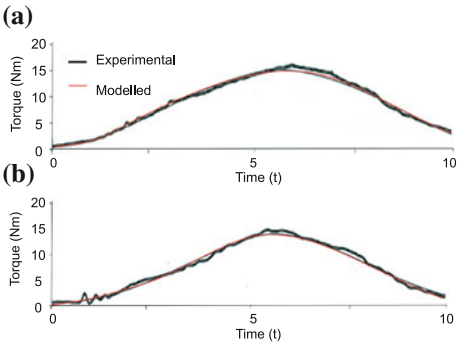

Fig. 2.6 Fitting results for: **a** torque component $\tau_{2,1}$ and modelled $h_1(u_1, t)$ corresponding to isometric anterior deltoid muscle, and **b** torque component $\tau_{5,2}$ and modelled $h_2(u_2, t)$ corresponding to isometric triceps muscle

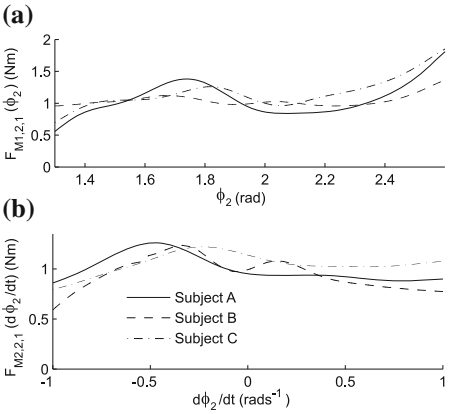

Fig. 2.7 Fitting results for: **a** $F_{M1,2,2}(\phi_2)$ and **b** $F_{M2,2,2}(\dot{\phi}_2)$

$$h_{IRC,1}(u_1) = a_{1,i}\frac{\exp(a_{2,i}u_1) - 1}{\exp(a_{2,i}u_1) + a_{3,i}}, \quad \text{and } h_{LAD,1}(t) = \mathscr{L}^{-1}\left\{\frac{w_{n,i}^2}{s^2 + 2w_{n,i}s + w_{n,i}^2}\right\}$$

have been taken for $i = 1, 2$.

Finally, multiplicative muscle functions of the form (2.20) have been identified through application of the procedure of Sect. 2.2.4. Results are given in Fig. 2.7. Note that since axes are aligned with muscle moments, all components of $F_M(\cdot)$ are zero apart from $F_{M,2,1}(\cdot)$ and $F_{M,5,2}(\cdot)$. Further results and fitting accuracy data can be found in [18, 21] for the case of both unimpaired and stroke participants.

2.3 Conclusions

This chapter has introduced general structures that model the dynamic response of the mechanically supported, electrically stimulated, upper limb. Identification procedures have been proposed and representative experimental results presented for the case of a passive exoskeletal support. In the next two chapters the general model form of (2.6) is used to design controllers which enable a reference tracking task to be completed. Chapter 5 then employs these model and controller structures within a clinical intervention to assist stroke patients' completion of upper limb reaching tasks.

References

1. J. Mehrholz, A. Hadrich, T. Platz, M. Pohl, Electromechanical and robot-assisted arm training for improving generic activities of daily living, arm function, and arm muscle strength after stroke. Cochrane Database Syst. Rev. **6**, CD006876 (2012)
2. P.S. Lum, C.G. Burgar, P.C. Shor, Evidence for improved muscle activation patterns after retraining of reaching movements with the mime robotic system in subjects with post-stroke hemiparesis. IEEE Trans. Neural Syst. Rehabil. Eng. **12**(2), 186–194 (2004)
3. J.R. de Kroon, J.H. van der Lee, M.J. Ijzerman, G.J. Lankhorst, Therapeutic electrical stimulation to improve motor control and functional abilities of the upper extremity after stroke: a systematic review. Clin. Rehabil. **16**, 350–360 (2002)
4. J.H. Burridge, M. Ladouceur, Clinical and therapeutic applications of neuromuscular stimulation: a review of current use and speculation into future developments. Neuromodulation **4**(4), 147–154 (2001)
5. E.K. Chadwick, D. Blana, A.J. van den Bogert, R.F. Kirsch, A real-time, 3-d musculoskeletal model for dynamic simulation of arm movements. IEEE Trans. Biomed. Eng. **56**(4), 941–948 (2009)
6. D. Blana, J.G. Hincapie, E.K. Chadwick, R.F. Kirsch, A musculoskeletal model of the upper extremity for use in the development of neuroprosthetic systems. J. Biomech. **41**, 1714–1721 (2008)
7. D. Zhang, T.H. Guan, F. Widjaja, W.T. Ang, Functional electrical stimulation in rehabilitation engineering: a survey, in *Proceedings of the 1st International Convention on Rehabilitation Engineering and Assistive Technology*. ACM (2007), pp. 221–226
8. F.J. Valero-Cuevas, A mathematical approach to the mechanical capabilities of limbs and fingers. Prog. Mot. Control **629**, 619–633 (2009)
9. B. Doran, A.K. Thompson, R.B. Stein, Short-term effects of functional electrical stimulation on spinal excitatory and inhibitory reflexes in ankle extensor and flexor muscles. Exp. Brain Res. **170**(2), 216–226 (2006)

10. D. Zhang, W.T. Ang, Musculoskeletal models of tremor (chapter 5), *Mechanisms and Emerging Therapies in Tremor Disorders* (Springer Science & Business Media, Berlin, 2012), pp. 79–107
11. J. Bobet, E. Gossen, R. Stein, A comparison of models of force production during stimulated isometric ankle dorsiflexion in humans. IEEE Trans. Neural Syst. Rehabil. Eng. **13**(4), 444–451 (2005)
12. J. Bobet, R. Stein, A simple model of force generation by skeletal muscle during dynamic isometric contractions. IEEE Trans. Biomed. Eng. **45**(8), 1010–1016 (1998)
13. J. Ding, A.S. Wexler, S.A. Binder-Macleod, A mathematical model that predicts the force frequency relationship of human skeletal muscle. Muscle Nerve **26**(4), 477–485 (2002)
14. L.A. Law, R.K. Shields, Mathematical models of human paralyzed muscle after long-term training. J. Biomech. **40**(12), 2587–2595 (2007)
15. E.-W. Bai, Z. Cai, S. Dudley-Javoroskv, R.K. Shields, Identification of a modified Wiener-Hammerstein system and its application in electrically stimulated paralyzed skeletal muscle modeling. Automatica **45**, 736–743 (2009)
16. C.T. Freeman, Upper limb electrical stimulation using input-output linearization and iterative learning control. IEEE Trans. Control Syst. Technol. **23**(4), 1546–1554 (2015)
17. J. Yu, D.C. Ackland, M.G. Pandy, Shoulder muscle function depends on elbow joint position: an illustration of dynamic coupling in the upper limb. J. Biomech. **44**(10), 1859–1868 (2011)
18. C.T. Freeman, A.M. Hughes, J.H. Burridge, P.H. Chappell, P.L. Lewin, E. Rogers, A model of the upper extremity using FES for stroke rehabilitation. ASME J. Biomech. Eng. **131**(3), 031006–1–031006–10 (2009)
19. F. Le, I. Markovsky, C.T. Freeman, E. Rogers, Identification of electrically stimulated muscle models of stroke patients. Control Eng. Pract. **18**(4), 396–407 (2010)
20. W.K. Durfee, K.I. Palmer, Estimation of force-activation, force-length and force-velocity properties in isolated, electrically stimulated muscle. IEEE Trans. Biomed. Eng. **41**(3), 205–216 (1994)
21. D. Tong, Upper limb rehabilitation system using FES mediated by ILC. Ph.D. thesis, University of Southampton (2013)

http://www.springer.com/978-3-319-25704-4

Control System Design for Electrical Stimulation in Upper Limb Rehabilitation
Modelling, Identification and Robust Performance
Freeman, C.
2016, XIII, 176 p., Hardcover
ISBN: 978-3-319-25704-4